Microscopy (TEM and SEM) and GIF (Gatan Image Filtering) element mapping of alkali feldspars replacing plagioclase in granitic rocks shows that the hematite precipitates are sub-micron sized and related to K-feldspar replacing plagioclase, associated with pore formation in the K-feldspar. In the neighborhood of the replacement front an amorphous region of non-stoichiometric minerals can be found. In this study a sample of fenno-scandian pink granite was prepared for optical, SE and TE Microscopy analysis. Optical petrography reveals regular grain size and a mineral assemblage that consists mostly of plagioclase, K-feldspar, quartz and biotite. Abundant tiny inclusions in the feldspar can be seen in optical analysis, but can only be identified as iron bearing minerals in the SEM, using EDX. For TEM analysis, the polished thin sections were further thinned using a Gatan ion-mill. In the TEM, copious iron-bearing needle-like minerals can be found spatially related to minute pores. Selected Area Electron Diffraction (SAED) patterns identify hematite. Figure 2 shows an example of a hematite needle embedded in K-feldspar. The zero-loss image shows a sharp contrast of the iron-bearing needle against the silicate matrix. The thickness map and profile show that the sample is wedge shaped – from 1.5 to 0.5 lambda (lambda is the mean free path for plasmon generation in the material [2]). In thinner parts of the natural feldspar sample abundant pores can be found, but in very few of them the hematite needles are preserved. In thicker parts, the nearest neighborhood of many pores contains hematite needles. The needle is usually thicker then the surrounding matrix, an effect partly due to preferential thinning of the silicates in the ion mill. In figure 3 several element distribution maps are shown. They were obtained by the "three window method" [2], using a GIF coupled to a JEOL 3010 TEM. The needle is clearly discernible in the iron map, but some iron is also present in the amorphous material around the needle. Potassium concentration is enhanced in the immediate vicinity of the needle, sodium is also present in the same area as K, but does not show so many concentration gradients. Ca distribution is complementary to the alkali distribution, indicating the replacement of the Ca-containing plagioclase. The precipitation of hematite at pores and the non-crystalline regions at the transformation boundary allows interpretation of a precipitation like mineral reaction [3]. The common occurrence of red feldspars in large granitic bodies and the association of red coloration to pore-related hematite imply that large scale fluid enhanced metasomatic processes contribute to coloration of the whole granite body.

References:

[1] G.M. Boone, Origin of clouded red feldspars: petrologic contrasts in a granitic porphyry intrusion. Am.J. Sci. 267, (1969) 633-668.

[2] R.F. Egerton , Electron Energy-Loss Spectroscopy in the Electron Microscope: Plenum Press (1989) Second Edition

[3] P.M. Orville, Plagioclase cation exchange equilibria with aqueous chloride solution: results at 700°C and 2000 bars in the presence of quartz, Am. J. Sci. 272 (1972) 234-272.

HEAVY METALS IDENTIFICATION IN ALLUVIUM SEDIMENTS FROM RIBEIRA DE IGUAPE RIVER - BRASIL

Jesus, S. L.[1];Guimarães, V.[2]; Sigolo, J. B.[2]
[1]Núcleo de Pesquisas em Geoquimica e Geofísica da Litosfera
- NUPEGEL/ESALQ/USP
[1,2]Instituto de Geociências – IGC/USP

Heavy metals reach net drains mainly from mining effluents, industry and domestic sewage, which the first ones are, the main fonts of contamination. Mining potentially leaves heavy metals to ambient since disrupt geochemical equilibrium of material rich of these elements with tendency to react with other compartments (hydrosphere, atmosphere and biosphere) and transported or transformed, causing damage effects even stopping emission. Hydrographic basin of Ribeira de Iguape, localized in São Paulo and Paraná States receive the flushing of heavy metals (Pb, Ba, Zn, As, Cu, Ag, Cr and Cd) from processing of various mines (scrap mining) as well metallurgical factory (slag) to their drains including hole medium down part of Ribeira de Iguape River up to lacuna estuarine system Iguape-Cananéia [1, 2 and 3] so that this residues were marginal accumulated as deposits along the river. These work aim evaluating concentration of heavy metals in alluvium sediments of Ribeira de Iguape River. Nine profiles of alluvium sediments along the segment Iporanga-Eldorado were collected which ones were subdivided at field in top, medium and base. Samples were homogenized and 2.00mm sieved and smaller fraction analyzed by x-ray fluorescence (XRF). Results were compared with reference values to sediments to Canadian Council of Minister of the Environment [4] and values of regional backgrounds, in accord to CPRN [5]. Complementary evaluations by scanning electron microscopy (SEM) Jeol 5600 LV attached with energy-dispersive spectrometer (EDS) Noram/Voyager were carried out, figure 1. With regard to Cr, Zn and Pb contents results indicated possible contamination area after compared data with international references (table 1, 2 and 3). This way, alluvium sediments show in their composition Pb, Zn and Cr came from of activities mines (mines at header) and this is unnatural occurrence since this values is over regional background references, an evidence that origin residues were came from launches in the river during 40 years mining.

References

[1] CETESB – Companhia de Tecnologia de Saneamento Básico, 1986 Avaliação dos níveis de contaminação por metais pesados e pesticidas organoclorados na água, ictiofauna e outros organismos aquáticos do complexo estuarino lagunar Iguape-Cananéia: Relatório final. São Paulo. 68pg.

[2] Moraes, R. P., 1997 Transporte de Chumbo e metais associados no rio Ribeira de Iguape, São Paulo. Campinas, 94pg. Dissertação de mestrado, Instituto de Geociências, Universidade Federal de Campinas.

[3] Tessler, M. G; Suguio, K.; Robiolotta, P. R.; 1987 Teores de alguns elementos traços metálicos em sedimentos peliticos da superficie de fundo da região lagunar de Cananéia-Iguape. In: Simpósio sobre ecossistemas da Costa Sul e Sudeste Brasileira: Sintese dos conhecimentos. Cananéia. Anais ACIESP. São Paulo, v.2, p.255-263.

[4] CCME – Canadian Council of Ministers of the Environment, 1999 Canadian sediment quality guidelines for the protection of aquatic life. http://www.ccme.ca/publications/can_guidelines.html.

[5] CPRN - Coordenadoria de Proteção dos Recursos Naturais. 1978 Relatório técnico: Projeto geoquímico no vale do Ribeira – Relatório final. São Paulo. 326pg.
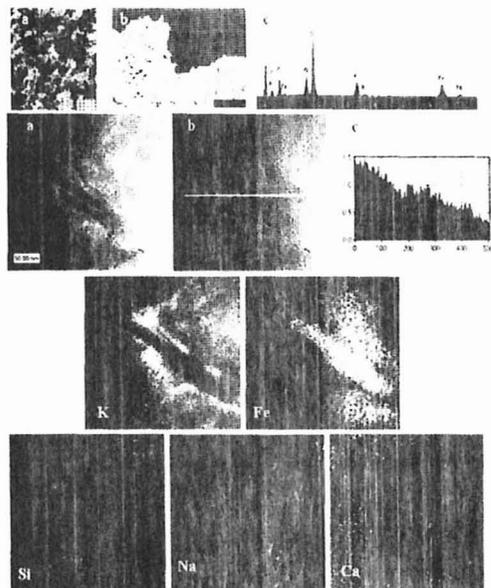

Figure 1 - (a) The optical image shows a fenno-scandian granite with red clouded feldspars. (b) The backscattered electron image shows the boundary between plagioclase (dark grey) and K-feldspar (light grey). Abundant bright spots in the porous K-feldspar were identified as hematite precipitates, by (c) EDX spectroscopy. Figure 2 (a) EFTEM zero-loss imaging of a hematite needle in K-feldspar, (b) Thickness map of the same area and (c) thickness profile of indicated line in units of mean free path (lambda). Figure 3 Element mapping of the region of Figure 2 using GIF "three windows method". Same scale as in Figure 2(a)

Elements ppm	11.91 (Topo)	12.92 (Topo)	11.025.92 (Topo)	11.03 (Topo)	11.04 (Topo)	11.05 (Topo)	11.06 (Topo)	11.07 (Topo)	11.08 (Topo)	11.09 (Topo)			Background Regional
Cr	340.00	244.57	560.00	250.37	0.00	0.00	330.52	0.00	0.00	0.00		90.00	37.30
Zn	40.00	62.31	63.32	63.32	65.00	0.00	58.43	0.00	0.00	0.00		315.00	123.00	47.00
Pb	53.00	45.60	63.32	73.92	89.26	133.00	67.89	61.35	21.50	21.50		81.36	35.00	16.00

Elements (ppm)	19.02 (Meio)	19.025.02 (Meio)	11.03 (Meio)	11.03 (Meio)	11.06 (Meio)	11.07 (Meio)	11.08 (Meio)	11.09 (Meio)			Background Regional
Cr	340.00	261.00	159.00	630.00	273.00	0.00	0.00	0.00		90.00	37.30
Zn	31.92	20.00	63.32	160.00	0.00	0.00	0.00	0.00		315.00	123.00
Pb	5.00	106.00	63.26	130.00	89.26	0.00	0.00	0.00		81.15	35.00	16.00

Elements (ppm)	11.025.02 (Base)	11.03 (Base)	11.05 (Base)	11.06 (Base)	11.07 (Base)	13.08 (Base)	13.09 (Base)			Background Regional
Cr	340.00	261.57	630.00	544.00	456.96	347.48	712.00	90.00		37.30
Zn	60.00	55.68	160.00	160.00	453.99	58.43	77.00	315.00	123.00	47.00
Pb	53.00	64.73	63.00	196.00	89.26	67.89	69.35	81.35	35.00	16.00

Table 1- Contents of metals detected in samples collected in top profile of alluvium sediment at Iporanga-Eldorado segment. Table 2- Contents of metals detected in samples collected in medium profile of alluvium sediment at Iporanga-Eldorado segment. Table 3- Contents of metals detected in samples collected in base profile of alluvium sediment at Iporanga-Eldorado segment.
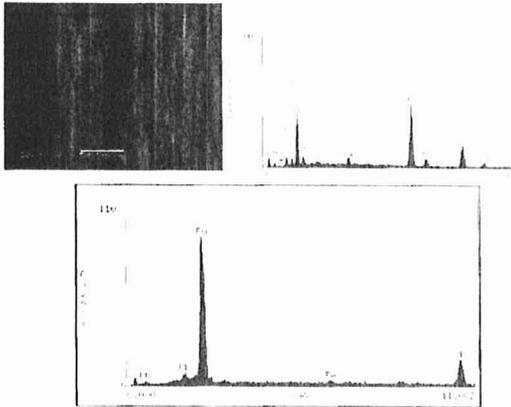

Figure 1: micrograph of sediments and energy-dispersive analysis.

MICROANALYSIS OF HUMIC SUBSTANCES USED FOR SOIL RECOVERY AND WASTE TREATMENT

Mauricio, M. H. P.*; Faller, M. C. K.; Joubert, E.; Brocchi, E. A.; Nunes, R. A.
Pontifícia Universidade Católica do Rio de Janeiro
Departamento de Ciência dos Materiais e Metalurgia
*e-mail: marcoshta demm.puc-rio.br

Humic substances are extremely widespread in nature, distributed in aquatic and soil environments, such as caustobioliths, oil shales, fossil coals, brown coal, as well as in fluvial and marine clastic deposits. The most important humic substances (HSs) content are the humic acids (HAs), which are high-molecular aromatic organic compounds with few tens of acidic groups, as shown in Figure 1. Some of the most important properties of HAs are their absorptive, flocculating, and structurizing capacities [1]. This set of valuable properties has been explored for the application of HAs in several ambiental problems [2]. There are a number of possible raw-materials for the production of commercial HSs, among them can be cited brown coal, peat and vegetal coal. Recently, an interdisciplinary research group has been built up at PUC-Rio to study the potential applications of the humic substances in soil recovery and in waste and water treatments. The main interests are to provide solutions for solid and liquid waste from mining and industrial activities as well as to recover spoiled areas. For this purpose, some preliminary investigations were carried out using some different HSs formulations [3,4,5,6]. In the present work, three specific formulations of humic substances (called from now on as: HS 1, HS 2 and HS 3) produced by a Russian company (EPhAT Ltd), in a joint program with PUC-Rio, were microanalysed. Two of them (HS 1 and 2) were obtained from brown coal while the other (HS 3) was produced from a Brazilian charcoal (eucalypt tree). Then, the aim of this study is to contribute for a better comprehension of the behavior observed for each of those formulations in the previous [4,5] and undergoing experiments. The morphology of the HSs

aggregates and the main constituent elements were determined by scanning electron microscopy (SEM) and by EDS respectively. Samples of each HSs formulation were dried at 60°C during 24 hours. Then, the dry HSs agglomerates were spread over stubs and covered with a gold film for the SEM analysis. Typical SE images of the HSs are shown in Figure 2 and 3. The morphological differences between the agglomerates are very clear. Even when high magnification is used, the aggregate surfaces appearance are quite different. Therefore, their morphological aspects can aid to explain an HSs different behavior [5] whenever they were used under the same experimental conditions. Meanwhile, the EDS spectra, as shown in Figure 4, indicate the presence of the same elements (Si, Fe, Al, Ca and K) in the HSs produced from brown coal. These elements are characteristic of humic substances from mineral coal. In the case of the HS produced from vegetal coal only Ca was detected. The microanalysis studies will now support the undergoing researches. These have indicated that, as aiming the water recycling, HS 1 has a better response to chelate metal ions and to reduce faecal coliforms, both in waste water. Besides, HS 1 has presented greater coagulation capability, as can be pointed out by the images showing large agglomerates (Figure 2a). The HS 2 has prospective applications in soil recovery, as adsorbing agent of toxic organic compounds (as TCE, BTX, etc.). Finally, the HS 3 has possibly a high cationic sorption capability, which could be explained by the presence of more active sites, since only Ca was detected in its structure (Figure 4c).

References:

[1] Davies, G. and Ghabbour, E. A., Humic Substances: Structures, Properties and Uses, Royal Society of Chemistry, Cambridge, 1998.

[2] Kochany, J. and Smith, W., Proceedings of Waste Management 2001 Conference (2001). www.wmsym.org/Abstracts/2001/43A/43A-10.pdf

[3] Mauricio, G. M.; Nunes, R. A.; Benites, V. M. In: XII International Meeting of the International Humic Substances Society, Humic Substances and Soil and Water Environment (2004), p. 321-323.

[4] Shulgin, A.; Nunes, R. A.; Brocchi, E. A.; Faller, M. C. K., In: XII International Meeting of the International Humic Substances Society, Humic Substances and Soil and Water Environment (2004),. p. 474-476.

[5] Nunes, R. A.; Shulgin, A.; Brocchi, E.A.; Faller, M. C. K., In: XII International Meeting of the International Humic Substances Society, Humic Substances and Soil and Water Environment (2004), p. 535-537.

[6] Mauricio, M. H. P.; Mauricio, G. M.; Nunes, R. A.; Shulgin, A., Resumos do V Encontro Brasileiro de Substâncias Húmicas (2003).
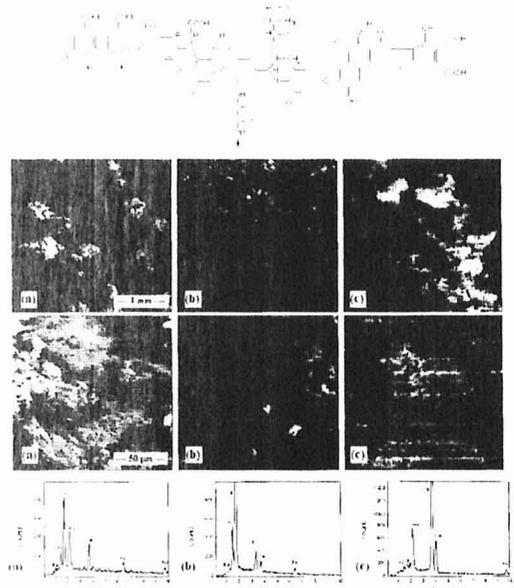

Figure 1 — Molecular structure of humic acid. Figure 2 – SE images of 3 different HSs formulations. Magnification = 50X. (a) HS 1, (b) HS 2, (c) HS 3. Figure 3 – Same of Figure 2, with magnification = 1kX. Figure 4 – EDS spectra of: (a) HS 1, (b) HS 2, (c) HS 3.